

Constraining the extra heating of the Diffuse Ionized Gas in the Milky Way

T. Elwert¹ and R.-J. Dettmar

Astronomisches Institut, Ruhr-Universität Bochum, Universitätsstr. 150, D-44780 Bochum, Germany
 elwert@pa.uky.edu, dettmar@astro.rub.de

ABSTRACT

The detailed observations of the diffuse ionized gas through the emission lines $H\alpha$, [NII], and [SII] in the Perseus Arm of our Galaxy by the Wisconsin $H\alpha$ Mapper (WHAM)–survey challenge photoionization models. They have to explain the observed rise in the line ratios [NII]/ $H\alpha$ and [SII]/ $H\alpha$. The models described here consider for the first time the detailed observational geometry toward the Perseus Arm. The models address the vertical variation of the line ratios up to height of 2 kpc above the midplane. The rising trends of the line ratios are matched. The increase in the line ratios is reflected in a rise of the temperature of the gas layer. This is due to the progressive hardening of the radiation going through the gas. However an extra heating above photoionization is needed to explain the absolute values. Two different extra heating rates are investigated which are proportional to n^0 and n^1 . The models show that a combination of both are best to explain the data, where the extra heating independent of density is dominant for $z > 0.8$ kpc.

Subject headings: radiative transfer, methods: numerical, Galaxy: halo, ISM: structure

1. Introduction

Containing typically half the mass of ionized hydrogen in galaxies, the Diffuse Ionized Gas (DIG) is visible as an extended $H\alpha$ emitting layer in our Galaxy (e.g. the WHAM–survey) and in many other galaxies (see e.g. Tüllmann & Dettmar (2000), Collins & Rand (2001), Otte et al. (2001), Hoopes & Walterbos (2003)). Studies of emission line ratios such as [NII]/ $H\alpha$ and [SII]/ $H\alpha$ provide information about the physical conditions of the gas. Simple energy estimations (Reynolds (1990), Reynolds (1993)) favor O and early B stars to be responsible for most of the DIG. 3D models using various methods (e.g. Miller & Cox (1993), Dove & Shull (1994), Wood & Loeb (2000), Ciardi et al. (2002), Wood et al. (2004)) showed that it is possible for ionizing photons from O stars to penetrate from the midplane into the halo. Wood & Mathis (2004) noted that the line

ratios increase with distance from the midplane due to the progressive hardening of the radiation. So far photoionization models made no specific attempt to model the trends of the line ratios. Models by Mathis (2000), Domgörgen & Mathis (1994), Sembach et al. (2000), Bland–Hawthorn et al. (1997) used volume average models to explain the observed data. The analytical approach by Haffner et al. (1999), referred to as Haffner99 in the rest of this paper, treated the dependence of the line ratios with height. Haffner99 and its further application to other galaxies by e.g. Collins & Rand (2001), Otte et al. (2001), and Miller & Veilleux (2003) gave evidence that an additional heating source is needed in order to explain the rise of the line ratios with increasing distance z from the midplane.

We are constructing photoionization models in order to examine the trends in the observed line ratios and if photoionization can heat up the gas sufficiently in order to explain the data. We introduce specific extra heating terms, extra means

¹present address: Department of Physics and Astronomy, University of Kentucky, Lexington, KY 40506, USA

in addition to photoionization, and discuss their properties. In the following section 2 we introduce the observations of the Perseus Arm to which our models are compared. Section 3 deals with the model parameters and discusses geometry and sight line effects taken into account. The models are compared with the data in the next section. The last section summarizes the results.

2. Data of the Perseus Arm

We are using the data taken from the Wisconsin H α Mapper (WHAM) (e.g. Haffner99, Haffner et al. (2003)) survey which were kindly provided by Ron Reynolds and Matt Haffner. The WHAM-survey mapped the northern sky in H α with declinations of $\delta > -30^\circ$. The Perseus Arm ($-35^\circ < \delta < -11^\circ$ and $120^\circ < l < 150^\circ$) was additionally mapped in [NII] λ 6583 and [SII] λ 6716. At each pointing an averaged spectrum with a beam of 1° is measured with a velocity resolution of 12 km s^{-1} . The emission of the Perseus Arm can be separated in velocity space from the local emission (Haffner99) for galactic longitudes $120^\circ < l < 150^\circ$. This was performed by integrating the line emission in the velocity range $-100 \text{ km s}^{-1} < v < -20 \text{ km s}^{-1}$, no line fitting was performed. We are using the intensity of the H α line as well as the line ratios [NII]/H α and [SII]/H α . The sensitivity limit of 0.1 Rayleighs^1 results in an observed vertical height of up to $|z| = 2 \text{ kpc}$ assuming a distance to the arm of 2.5 kpc .

3. Model parameters

We use the spectral simulation code CLOUDY, version 96.00 (described by Ferland (2002), (2000), (1998)) to model the DIG. CLOUDY determines the physical conditions by balancing the heating and cooling rates, so that the energy is conserved. The results of the models are compared to the observed emission line ratios [NII]/H α and [SII]/H α , and the gas temperature as derived from [NII]/H α .

In order to realize a model describing the DIG certain parameters have to be specified: The ionizing spectrum of the source is a composition of three different stellar temperature: 56% from $T = 35000 \text{ K}$, 12% from $T = 40000 \text{ K}$, and 32% from $T = 45000 \text{ K}$, as used in Mathis (2000) and Wood

et al. (2004). The WMbasic models (Pauldrach et al. (2001)), which include N-LTE effects, X-ray emission from shocks within stellar winds, are used as the ionizing spectra. The luminosity of the source is chosen in such a way that the observed run of the H α intensity is matched, as shown in Figure 1.

The density structure is exponential, as derived from the observed H α intensity, with a scale height of 1 kpc and a midplane density of 0.2 cm^{-3} . The density is in clumps with a filling factor of 20%, i.e. only 1/5 of the volume is filled with this plasma. The geometry of the ionized gas is chosen to be a plane parallel layer, i.e. the ratio of the depth of the cloud to the distance of the illuminated face to the ionizing source is smaller than 1/10.

We are matching the observed H α intensity of the observations (Figure 1) by placing the illuminated face of the cloud at a z -height of 1 scale height of the Lockman-layer (300 pc) assuming a density law of $n = 0.1 \exp(-z/0.3)$ as in Miller & Cox (1993). This is done after the model is calculated as otherwise the condition of plane parallel illumination of the cloud cannot be fulfilled. The information of the actual position of the ionizing stars are effectively removed, consistent with the picture of having the DIG being ionized by radiation leaking out of the Lockman-layer. The intensity gradient of H α is matched as well as the estimate of the hydrogen ionizing photon flux by Reynolds (1990): $\phi_{DIG} \geq 5 \times 10^6 \text{ hydrogen ionizing photons cm}^{-2} \text{ s}^{-1}$. In order to compare the models on a common basis, which is important as extra heating is dominating for large z -heights, we choose to let the ionization structure be the same for all models (see Figure 5). This is in accordance with the idea that the extra heating affects only the temperature of the gas. The forbidden levels of nitrogen and sulphur can then be more easily excited by collisions with the electrons which in turn elevates the line ratios [NII]/H α and [SII]/H α . Figure 1 shows that the intensity gradient of H α varies only a little for the different models. The scale heights for the models are slightly different ($\ll 10\%$) for the models with an extra heating, which can be explained by assuming that the DIG-layer is in pressure equilibrium. This effect was also noted by Wood & Mathis (2004). The ionization parameters (U) of all models lie in the narrow range between $\log(U) = -3.0$ and -3.1 .

¹1 R = $10^6/4\pi \text{ photons cm}^{-2} \text{ s}^{-1} \text{ sr}^{-1}$

The ISM composition of CLOUDY is used with N/H and S/H set to the values in Haffner99 (N/H = 7.5×10^{-5} , S/H = 1.86×10^{-5}). Graphite and silicate grains with the size distribution used for the ISM (see HAZY, Ferland (2002)) are present in the gas and account for less than 10 % of the global heating. The inclusion of PAHs give only variations $< 3\%$ for the line ratios and have only a small effect on the heating balance. The interaction with cosmic rays is taken into account as described in Ferland & Mushotsky (1984).

A crucial factor is the consideration of the line of sight. The observations give information about the line ratios at different positions orthogonal to the source of the ionizing radiation. The correct local line ratios are represented by the ratios of the volume emission coefficients ϵ_V : $\frac{I_1}{I_2} = \frac{\int dz \epsilon_{V_1}}{\int dz \epsilon_{V_2}} \approx \frac{\epsilon_{V_1}}{\epsilon_{V_2}}$. An important issue is the treatment of the line of sight to the Perseus Arm due to our position in the Milky Way as shown in Fig. 2. Each pointing of the WHAM survey contains contributions from different $|z|$ heights above the midplane ($\epsilon(z1)$ to $\epsilon(z2)$), this effect is taken into account by integrating over the particular sight line in the models. The distance to the Perseus Arm is assumed to be 2.5 kpc and the thickness of the arm to be 1 kpc as quoted in Haffner99. Moreover, the observations are the average of a beam size of 1° which means that we have to take into account an additional integration over different z heights, on average 45 pc. These effects of geometry and observational smearing are taken into consideration here for the first time. Fig 3 shows the effect of the beam smearing and line of sight geometry on the calculated line ratios for z -heights up to 2.5 kpc, which have to be considered for the observed heights of 1.8 kpc. These effect increase the 'corrected' line ratios by at most 15% and their trend is altered for high z -heights. The 'corrected' model without an extra heating seems to suggest that [NII]/H α is not increasing after about 1.6 kpc, but the 'uncorrected' model shows a further increase due to the hardening of the radiation. The result of the gas temperature (section 3.2, Fig. 4) is even more influenced by this issue. The discussion of the line ratios therefore need to include an appropriate treatment of the line of sight geometry and the beam smearing to

take these effects into account.

3.1. Extra heating

Additional heating to photoionization is included which is proportional to n^1 and n^0 in accordance with Reynolds et al. (1999), their factors G_1 and G_2 respectively. We choose rates in the same range as in their paper: $G_1 = 1 \times 10^{-25} \text{erg cm}^{-3} \text{s}^{-1}$ and $G_2 = 5 \times 10^{-27} \text{erg cm}^{-3} \text{s}^{-1}$. The heating-cooling balance can then be written as either $G_0 + G_1/n_e = \Lambda$ or $G_0 + G_2/n_e^2 = \Lambda$. The heating due to photoionization is given by $G_0 n_e^2$ and the cooling by Λn_e^2 . The inclusion of an extra heating source rises the gas temperature of the models, at the same time the ionization structure varies only slightly. The temperature of the CLOUDY models are calculated by heating-cooling balance. The extra heating therefore increases the temperature, having more pronounced effects at larger z heights as the photoionization heating rate decreases like n^2 as shown in Fig. 4. The graph is explained in more detail in the next section.

In our models the ionization structure is nearly unaffected by the inclusion of an extra heating source, sulphur is slightly more effected than nitrogen. This behavior is the basic assumption for the extra heating in Reynolds et al. (1999). However they are assuming a constant ratio of N^+/N , whereas the models show a dependence on z height, this is expected as the radiation gets progressively absorbed. Figure 5 shows ionization structure and the change dependent on the different heating rates. Hydrogen is nearly fully ionized throughout all models which is a basic characteristic of the DIG.

3.2. Comparison with Observations

In Fig. 6 and Fig. 7 the models differ by the type of extra heating, ranging between models without extra heating and a rate of $G_1 = 1 \times 10^{-25} \text{erg cm}^{-3} \text{s}^{-1}$ and $G_2 = 5 \times 10^{-27} \text{erg cm}^{-3} \text{s}^{-1}$. There was no fitting done in order to match the models with the observations. No 'best-fit' exists and therefore the models are independent of the observational quality, individual spectral features, or small scale variations which cannot be reproduced with a smooth density distribution. As the data for small $|z|$ heights are contaminated

with radiation from the midplane and dust absorption it is convenient to consider line ratios for $|z|$ -heights above 0.8 kpc to be 'pure' DIG. This is also the range for which the $H\alpha$ scale height was determined. The models show lower values of $[\text{NII}]/H\alpha$ and $[\text{SII}]/H\alpha$ for the lower z heights as doubly ionized nitrogen contributes 35% and doubly ionized sulphur even 80%, as seen in Fig. 5. As a consequence $[\text{NII}]$ and $[\text{SII}]$ are weaker. Figure 6 shows the development of the line ratios with $|z|$ height, both the data and the models show an increase with $|z|$. The trend in the line ratios is matched by the models even without an extra heating source.

The $[\text{NII}]/H\alpha$ line ratio above 1 kpc can be explained with the models including an extra heating rate. The modeled $[\text{SII}]/H\alpha$ ratio is up to a factor of two below the observations, however the theoretical uncertainty for the $[\text{SII}]$ line is very high as dielectronic recombination is an important process in the DIG. As the corresponding recombination coefficients are not known (see discussion in Ferland et al. (1998)), the results of the models have to be handled with care. Our models use the KLUDGE approximation (Ferland (2002)). Models without dielectronic recombination have $[\text{SII}]/H\alpha$ decreased by 50%. If the rate is doubled then $[\text{SII}]/H\alpha$ is increased by 50%.

Figure 4 shows the gas temperature of the models, the increase of the line ratios with z height is due to the progressive hardening of the radiation as the photons go through the gas layer. In order to explain the observed line ratios an extra heating source is however needed which does not alter the general shape of the predicted line ratios but elevates the line ratios. As $[\text{NII}]$ and $[\text{SII}]$ are forbidden lines which get collisional excited by electrons, an increase in gas temperature increases the amount of electrons capable to excite the singly ionized nitrogen and sulphur ions which can then decay by emitting the emission lines in questions. The gas temperature is deducted from the observations through the relation - following Reynolds et al. (1999): $\frac{I_{[\text{NII}]}}{I_{H\alpha}} = 1.84 \times 10^5 \left(\frac{N^+}{N}\right) \left(\frac{H^+}{H}\right)^{-1} T_4^{0.39} \exp(-2.18/T_4)$. Assuming that $N^+/N = H^+/H$ and the abundance as stated in section 3 gives $\frac{I_{[\text{NII}]}}{I_{H\alpha}} = 13.75 T_4^{0.39} \exp(-2.18/T_4)$, $T_4 = T/10^4 \text{K}$. We are not using the collision strength of singly

ionized nitrogen from Reynolds et al. (1999): $N^+ : \Omega(^3P, ^1D) = 2.28 \cdot T_4^{0.026}$, Aller (1984), but the data from Stafford et al. (1994): $N^+ : \Omega(^3P, ^1D) = 3.02 \cdot T_4^{-0.01}$. This leads to the different coefficients and temperatures on average 250 K below the values of Reynolds et al. (1999). For singly ionized sulfur we use the data from Lanzafame et al. (1993) instead of Aller (1984) as in Reynolds et al. (1999). The plot also shows the impact of the line of sight geometry and beam smearing as well as the consideration of the ionization structure of the models. As the line of sight leads to higher $[\text{NII}]/H\alpha$ ratios (up to 15%,) these effects, when accounted for, lower temperatures. The ionization structure, i.e. $N^+/N \approx H^+/H$ is only valid for $z > 800 \text{ pc}$, leads to higher estimates of the temperature. The combined effect is the elevation of the derived temperature for $z < 800 \text{ pc}$ and above that lower values by about 200 K. The models without an extra heating source have temperatures too low, an extra heating source independent of density shows very good agreement with the observed temperatures. The extra heating $\propto n^1$ seems to best fit the data up to 800 pc, then the extra heating $\propto n^0$ gives the best agreement for higher z values. The interpretation for the z heights $< 800 \text{ pc}$ have to be handled with care as this region is contaminated by radiation from the midplane and therefore the part responsible for the DIG emission is difficult to estimate. Magnetic reconnection (e.g. Birk et al. (1998)) or heating by cosmic rays through linear Landau-damping (Lerche & Schlickeiser (2001)) are possible processes producing a heating independent of density. As photoelectric heating from dust grains is $\propto n^1$, the data suggest that there is more dust present at z -heights below 800 pc than present in the models if this mechanism is responsible for the elevated temperature.

In Fig. 7 the line ratios $[\text{NII}]/H\alpha$ and $[\text{SII}]/H\alpha$ are plotted against each other. Values of $[\text{NII}]/H\alpha$ greater than 1, which cannot be explained by classical HII-region calculations, are reached with models using an extra heating source. Also in this case the extra heating independent of density is able to produce higher $[\text{NII}]/H\alpha$ ratios than the other therefore matching better with the data. The limits of Haffner99 for two constant S^+/S ratios (0.5 and 0.25) are also given. The ionization fractions of the models (see Fig. 5) are within

these two limits for $z > 0.6$ kpc. Together with the temperature plot (Fig. 4) the models match in all these direct and derived quantities with the data and agrees with the estimates of Haffner99 and Reynolds et al. (1999). The application to other galaxies shows that this diagram is also a valuable diagnostic for the chemical evolution (Elwert et al. (2004)).

4. Summary

We have shown that the observed trend of the line ratios $[\text{NII}]/\text{H}\alpha$ and $[\text{SII}]/\text{H}\alpha$ above the Galactic plane can successfully be explained by photoionization models including extra heating and considering the line of sight geometry. The observed values need an extra heating source which strength lies at the lower end of the predicted values of Reynolds et al. (1999) due to our models. At high z heights ($z > 800$ pc) an extra heating independent of density gives the best agreement with the data, whereas for smaller z heights an extra heating term $\propto n^1$ gives better results concerning the temperature. There is an intrinsically increase in the line ratios and the gas temperature due to the progressive hardening of the radiation. The extra heating terms are enhancing this trend and elevate the line ratios to the observed values. It is important to incorporate the observing geometry to the Perseus Arm into the models when comparing with the data. A discussion concerning models of observed line ratios in edge-on galaxies is given in Elwert (2003) and Elwert & Dettmar (2005).

This work was supported by DFG through SFB 591 and through Deutsches Zentrum für Luft- und Raumfahrt through grant 50 OR 9707. TE wants to thank Kenneth Wood and Ron Reynolds for helpful comments and enlightening discussions while writing the paper. We also want to thank the anonymous referee for making many very useful suggestions and comments which helped to improve the publication.

REFERENCES

Aller, L.H. 1984, *Physics of Thermal Gaseous Nebulae* (Dordrecht: Reidel)

Birk, G.T., Lesch, H., Neukirch, T. 1998, *MNRAS* 296, 165

Bland–Hawthorn, J., Freeman, K.C., Quinn, P.J. 1997, *ApJ* 490, 143

Ciardi, B., Bianchi, S., Ferrara, A. 2002, *MNRAS* 331, 463

Collins, J.A., Rand, R.J. 2001, *ApJ* 551, 57

Domgörgen, H., Mathis, J.S. 1994, *ApJ* 428, 647

Dove, J.B., Shull, J.M. 1994, *ApJ* 423, 196

Elwert, T. 2003, Ph.D. Thesis, Ruhr–Universität Bochum

Elwert, T., Dettmar, R.–J. 2005, *ASPC* 331, 203, editor: Braun, R.

Elwert, T., Dettmar, R.–J., Tüllmann, R. 2003, *AAS*, 203, #111.05

Ferland, G.J. 2002, Hazy, A Brief Introduction to CLOUDY, Dept. Phys. Astron. Internal Rep. 96.00 (Lexington: Univ. Kentucky)

Ferland, G.J. 2000, *ASP Conference Proc.* Vol. 216

Ferland, G.J., Korista, K.T., Verner, D.A., Ferguson, J.W., Kingdon, J.B., Verner, E.M. 1998, *PASP* 110, 761

Ferland, G.J., Korista, K.T., Verner, D.A., Ferguson, J.W., Kingdon J.B., Verner, E.M. 1998, *PASP* 110, 761

Ferland, G.J., Mushotzky, R.F. 1984, *ApJ* 286, 42

Haffner, L.M., Reynolds, R.J., Madsen, G.J., Tuftte, S.L., Jaehning, K.P., Percival, J.P., Hausen, N.R. 2003, *ApJS* 149, 405

Haffner, L.M., Reynolds, R.J., Tuftte, S.L. 1999, *ApJ* 523, 223

Hoopes, C.G., Walterbos, R.A.M. 2003, *ApJ* 586, 902

Lanzafame, A.C., Tully, J.A., Berrington, K.A., Dufton, P.L., Byrne, P.B., Burgess, A. 1993, *MNRAS* 264, 402

Lerche, I., Schlickeiser, R. 2001, *A&A* 366, 1008

Miller, S.T., Veilleux, S. 2003, *ApJ* 592, 79

Miller, W.W. III, Cox, D.P. 1993, *ApJ* 417, 579

Mathis, J.S. 2000, *ApJ* 544, 347

- Otte, B., Reynolds, R.J., Gallagher III J.S., Ferguson, A.M.N. 2001, ApJ 560, 207
- Pauldrach, A.W.A., Hoffmann, T.L., Lennon, M. 2001, A&A 375, 161
- Reynolds, R.J. 1993, in AIP Conf. Proc. 278, Back to the Galaxy, ed. S.S. Holt & F. Verter, 156
- Reynolds, R.J. 1990, ApJ 349, L17
- Reynolds, R.J., Haffner, L.M., Tufte S.L. 1999, ApJ 525, L21
- Sembach, K.R., Howk, J.C., Ryans, R.S.I., and Keenan, F.P. 2000, ApJ 528, 310
- Stafford, R.P., Bell, K.L., Hibbert, A., Wijesundera, W.P. 1994, MNRAS, 268, 816
- Tüllmann, R., Dettmar, R.-J. 2000, A&A 362, 119
- Wood, K., Mathis, J.S. MNRAS 353, 1126
- Wood, K., Mathis, J.S., Ercolano, B. 2004, MNRAS 348, 1337
- Wood, K., Loeb, A. 2000, ApJ 545, 86

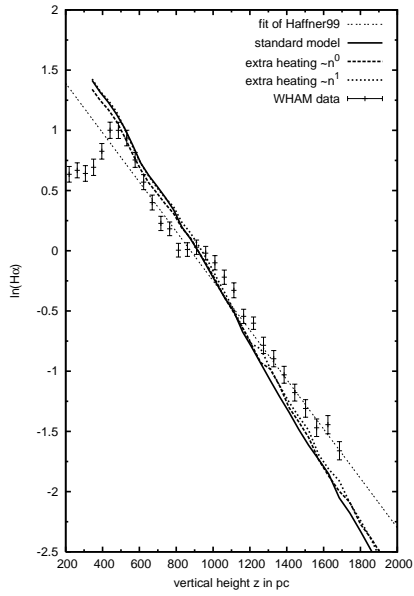


Fig. 1.— $H\alpha$ intensity of the Perseus Arm as observed by WHAM, overplotted is the fit of Haffner99 and the photoionization models with and without extra heating.

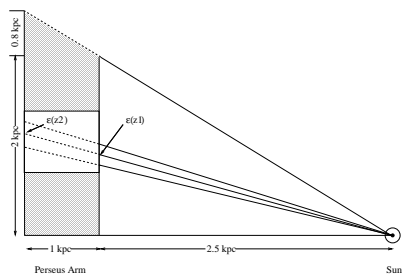


Fig. 2.— Sketch of the line of sight geometry and the beam smearing, which have to be considered when comparing the models with the data. Deriving temperatures from the data without taking this into account lead to temperatures that are on average 250 K higher.

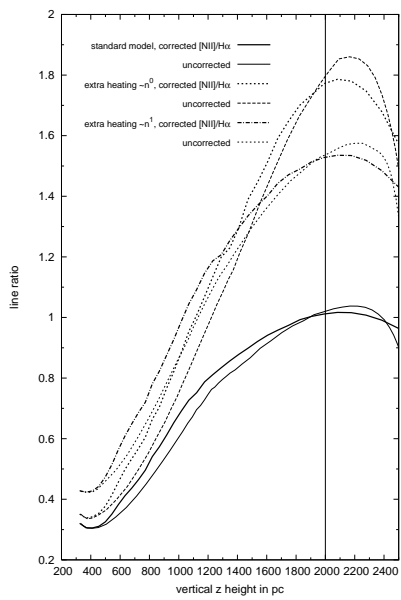


Fig. 3.— The effect of the beam smearing and line of sight geometry on $[\text{NII}]/\text{H}\alpha$ specifically. The enhancement of this line ratio due to this effect is at most 15% and leads to higher temperatures derived from the observations if the effects is not taken into account.

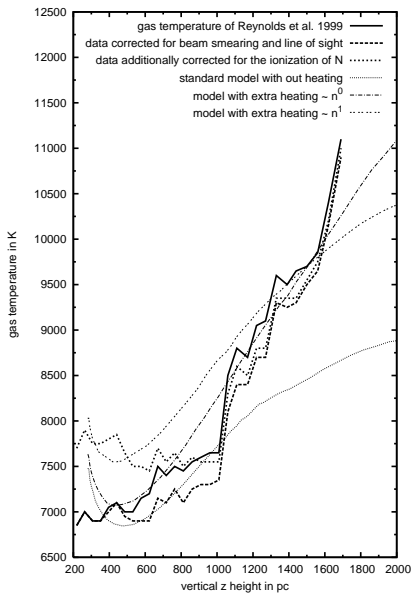


Fig. 4.— Temperature structure of the DIG, estimates from the observations with atomic data used by Stafford et al. (1994). The line of sight geometry and beam smearing lead to temperatures on average 250 K lower, whereas the consideration of the ionization structure of N^+ elevates the derived temperatures again. The figure shows that a combination of the two different heating terms gives the best agreement with the data.

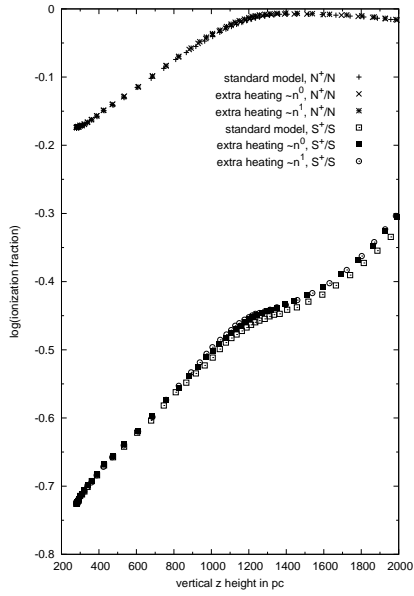


Fig. 5.— Ionization fractions of N^+ and S^+ dependent on z , the assumption of Haffner99: $N^+/N = H^+/H \rightarrow 1$ is approximately met for heights above 1300 pc.

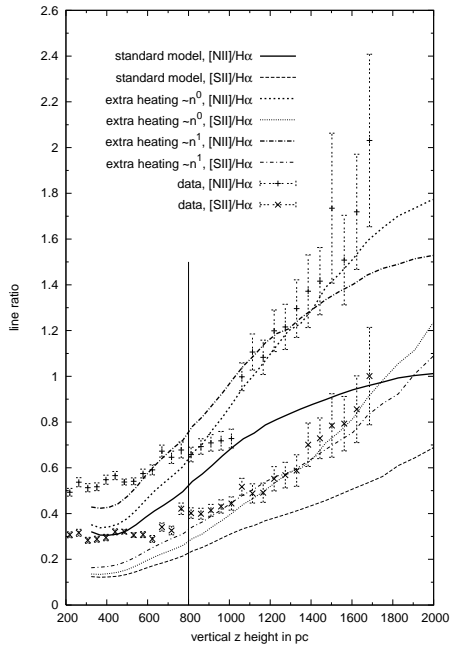


Fig. 6.— Observed [NII]/H α and [SII]/H α in the Perseus Arm, showing the characteristic rise. The models with and without an extra heating source are able to explain this trend, the explicit values are better reproduced with an extra heating.

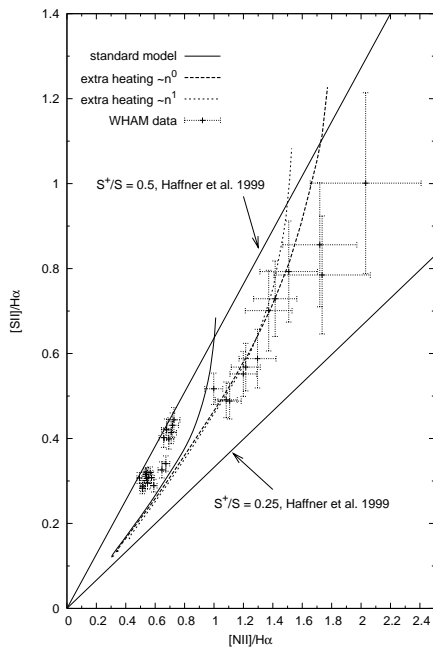


Fig. 7.— $[NII]/H\alpha - [SII]/H\alpha$ in the Perseus Arm as observed by WHAM, plotted are the models, the data, and the limits given by Haffner99 for two constant S^+/S ratios.